

University of Groningen

Low temperature dynamics in amorphous solids

Meijers, Hans C.; Wiersma, Douwe A.

Published in:
The Journal of Chemical Physics

DOI:
[10.1063/1.468321](https://doi.org/10.1063/1.468321)

IMPORTANT NOTE: You are advised to consult the publisher's version (publisher's PDF) if you wish to cite from it. Please check the document version below.

Document Version
Publisher's PDF, also known as Version of record

Publication date:
1994

[Link to publication in University of Groningen/UMCG research database](#)

Citation for published version (APA):
Meijers, H. C., & Wiersma, D. A. (1994). Low temperature dynamics in amorphous solids: A photon echo study. *The Journal of Chemical Physics*, 101(8), 6927-6943. <https://doi.org/10.1063/1.468321>

Copyright

Other than for strictly personal use, it is not permitted to download or to forward/distribute the text or part of it without the consent of the author(s) and/or copyright holder(s), unless the work is under an open content license (like Creative Commons).

The publication may also be distributed here under the terms of Article 25fa of the Dutch Copyright Act, indicated by the "Taverne" license. More information can be found on the University of Groningen website: <https://www.rug.nl/library/open-access/self-archiving-pure/taverne-amendment>.

Take-down policy

If you believe that this document breaches copyright please contact us providing details, and we will remove access to the work immediately and investigate your claim.

Downloaded from the University of Groningen/UMCG research database (Pure): <http://www.rug.nl/research/portal>. For technical reasons the number of authors shown on this cover page is limited to 10 maximum.

Low temperature dynamics in amorphous solids: A photon echo study

Hans C. Meijers and Douwe A. Wiersma

Ultrafast Laser and Spectroscopy Laboratory, Department of Chemistry, Materials Science Centre,
University of Groningen, Nijenborgh 4, 9747 AG Groningen, The Netherlands

(Received 15 April 1994; accepted 28 June 1994)

The long-lived stimulated photon echo is put forward as a powerful technique to probe structural dynamics in glasses and other amorphous solids. We present results of optical dephasing measurements on several doped organic glasses (deuterated ethanol, toluene, and triethylamine) and polymers (polystyrene, polyvinylbutyral, and polymethylmethacrylate). Using a stochastic analysis within the so-called two-level-system model, we can extract from these measurements the distribution function of fluctuation rates over a huge range of time scales, varying from picoseconds to hundreds of milliseconds. We show that the dynamics, which lies at the origin of spectral diffusion, is very dependent on the glass structure and can be described by two separate hyperbolic distribution functions of fluctuation rates. From longitudinal photon echo measurements in the population dimension, we find evidence for structural dynamics which is not accounted for in the standard two-level-system model and which is related to a spatially inhomogeneous distribution of fluctuation centers.

I. INTRODUCTION

Since Zeller and Pohl¹ reported that the low-temperature behavior of the specific heat and thermal conductivity in glasses is very different from crystals, many studies have been devoted to a better understanding of glasses. Glasses are solids, obtained by fast cooling of a liquid to an amorphous state. Although the disorder associated with the amorphous state varies from glass to glass, long range order is missing in all of them. Some glasses, however, show considerable short range order.^{2,3} Since electric and (nonlinear) optical properties of materials are much affected by energetic disorder, a fundamental study of amorphicity is also important from a technological point.

To account for the observed temperature dependence of the thermal conductivity and specific heat¹ in glasses, Anderson *et al.*⁴ and, independently, Phillips⁵ proposed the so-called two-level-system (TLS) model. A TLS can be pictured as a double well potential of which each well represents a distinct structural configuration of the glass. Changes in the glass structure are modeled by transitions from one well to the other. These transitions can even happen at very low temperature and are caused by phonon assisted tunneling. The glass is thought to consist of a large ensemble of these TLS's with a broad distribution of tunnel parameters and energy separations between the two levels, causing a broad distribution of fluctuation rates. Apart from being able to explain the anomalous temperature dependence of the thermodynamic properties of glasses, this model also predicts that these quantities will be time dependent, as has indeed been verified for the specific heat in amorphous silica.^{6,7} This dispersive time behavior traces back to a very broad distribution of tunneling rates of the two-level systems, ranging from THz to the inverse of the age of the universe. The underlying physical phenomenon is that glass dynamics not only comprises very fast fluctuations around an equilibrium structure, but also includes an evolution of the glass structure as a whole on a much slower time scale. Recently, a measurement of the thermal conductivity in an an-

cient natural glass (amber) revealed that this glass had undergone structural relaxation during the last 10^7 years, with a relaxation time of at least seven years.⁸

The TLS model has not only been successful in the description of the thermodynamic properties of glasses, but has also been used to account for the optical dynamics of guest molecules doped in glassy matrices. The first measurement on the optical homogeneous linewidth in a glass was performed by Selzer *et al.*⁹ using the fluorescence line narrowing technique. Soon thereafter, photon echoes¹⁰ and (nonphotochemical) hole burning experiments^{11,12} were also applied to study optical dephasing in amorphous solids. All these experiments showed a temperature dependence of the homogeneous linewidth, which was in between a linear and quadratic dependence on T . This sharply contrasts with a T^7 power law that was found in pure crystals¹³ and an exponential temperature dependence observed in molecular mixed crystals.¹⁴ In most hole burning experiments on organic glasses and polymers a $T^{1.3}$ power law was found,¹⁵⁻¹⁸ which was explained by assuming that the chromophore is dipolarly coupled to a bath of TLS's. The fractional power law then arises from a density of states that is nearly constant: $\rho(E) \propto E^{0.3}$.

Furthermore, it has recently been established that the homogeneous linewidth of a chromophore in a glass is also dependent on the time scale of observation, an effect that has not been observed in crystalline materials. The frequency of the optical transition continuously changes with the evolving glass dynamics and wanders, so to say, through frequency space. Because of these dispersive dynamics a separation of time scales between homogeneous and inhomogeneous broadening no longer exists, which violates one of the underlying assumptions of the optical Bloch equations. Glass dynamics, however, can still be described by the Bloch equations, provided that one allows the optical dephasing time constant to become time dependent: $T_2 = T_2(t)$. This time dependence of T_2 due to the frequency excursions of the optical dipole is generally referred to as "spectral diffusion."

The first actual measurement of a time scale dependent optical linewidth was reported by Breinl *et al.*,¹⁹ using photochemical hole burning. They observed in an alcohol glass that the hole width increases logarithmically with the time interval between burning and reading, which was varied from minutes to days. The Fayer group engaged in a thorough study of spectral diffusion by comparing photon echo and permanent hole burning experiments on several dyes in alcoholic glasses.²⁰ These studies provided firm evidence for the fact that considerable broadening of the "homogeneous" linewidth occurs between time scales of picoseconds and minutes. Thereafter, transient hole burning studies on ethanol and methyltetrahydrofuran (MTHF) glasses confirmed spectral diffusion to occur over times ranging from microseconds to hours.^{21,22} Stimulated photon echo experiments on the dye rhodamine 101 in PMMA revealed spectral diffusion on a nanosecond time scale.²³ Very recently, it has become possible to measure the changes of the transition frequency of one single molecule during times ranging from microseconds to hours. In these experiments support was found for the validity of a TLS model since it was observed that the optical transition frequency changes in discrete steps and shows indeed bistable behavior.^{24,25}

The commonly used theories of spectral diffusion heavily rely on a stochastic theory that was developed to describe phonon-echo and spin-echo decay in glasses.^{26–30} Hu and Hartman,²⁸ and later Hu and Walker,²⁹ analyzed spectral diffusion in terms of an uncorrelated sudden jump model for frequency fluctuations caused by flipping of TLS's. Later this theory was extended to the optical domain by Bai and Fayer,³¹ and exploited to extract the distribution of TLS relaxation rates from hole burning and photon echo experiments. Hayes and Small³² proposed that two types of TLS's exist: the nearby TLS_{ext}'s, which are intimately associated with the chromophore and held also responsible for nonphotochemical hole burning in glasses, and the intrinsic ones, TLS_{int}'s, being the pure glass TLS's, and which cause dephasing of the optical transition.

Detailed hole burning studies by Völker and co-workers³³ revealed that great care has to be taken when comparing dynamical information from different techniques like hole burning and photon echoes. Hole widths have to be extrapolated to zero burning fluence in order to correct for power broadening, which is intrinsic to the hole burning technique.³⁴ Furthermore, in all optical experiments very low laser powers have to be used to prevent heating of the sample because of the poor glass conductivity. It was also shown that optical linewidths can be influenced by the cooling history of the sample and that they may vary from sample to sample or even *within* one sample.^{33,35} The most reliable information on spectral diffusion can therefore only be gathered by a series of measurements on the same spot in the sample.

Since the homogeneous linewidth is broadened by the fluctuations in the glass, it is clear that a measurement of this linewidth as a function of time provides a unique opportunity to obtain insight in the time evolution of nonequilibrium glass structures. Such measurements will also be useful to a

study of the dynamics in other disordered materials such as proteins.^{36–39}

The ideal technique for a study of the time dependent homogeneous linewidth is capable of measuring the optical dynamics over a time range as large as possible. Although regular photon echo and hole burning methods have proven to be very powerful in the study of crystalline matrices, they have a disadvantage when applied to amorphous solids: The possible variation in the time scale of observation is rather limited. Photon echoes exclusively probe the very fast structural fluctuations that occur within the fluorescence lifetime (usually nanoseconds), while up to now hole burning can only be performed on timescales of microseconds or longer,^{22,40} leaving the time regime in between uncovered.

In a previous paper we have put forward an advanced echo technique, the long-lived stimulated photon echo,⁴¹ as a powerful probe of glass dynamics.⁴² The strength of this echo technique lies in the fact that the dephasing information can be stored for a much longer time compared to normal echoes by making use of an efficiently populated triplet state of the chromophore. The excited state population decays into this triplet state, which serves as a bottleneck. During the lifetime of this triplet state it is still possible to scatter an echo from the frequency grating that exists in the ground state. The time scale at which the photon echo decay is measured can now be varied in a continuous way from picoseconds (the regular two-pulse echo) to the lifetime of the bottleneck state, which, for a suitable chromophore, can be hundreds of milliseconds or even longer.

In this paper we report on the use of this technique for a study of structural dynamics in several organic glasses and polymers. Analysis of the measured echo decays yields the distribution function of the structural fluctuations in the glass over more than 11 decades of time, from THz down to at least 10 Hz. The technique is applied to several organic glasses and polymers and a comparison between the structural fluctuations occurring in these systems is made. We will present and discuss also measurements on the longitudinal decay of the stimulated photon echo, which provide an indication that a subset of chromophores is strongly coupled to nearby TLS's.

II. THEORETICAL BACKGROUND

When a stochastic model is used to describe the frequency modulation of a chromophore's transition due to coupling of the oscillator's transition dipole to the two-level systems in the amorphous solid, the intensity of the stimulated photon echo (three pulse echo or 3PSE) signal can be shown to be proportional to the square of the four-time correlation function.^{26,28,30,43}

Here, τ is the time interval between the first and second excitation pulses and t_w is the waiting time between the second and third pulses. N is the total number of TLS's in the volume V under consideration, while $\Delta\omega_j(t)$ represents the stochastic fluctuation of the optical transition frequency caused by the j th TLS.

$$I_{3\text{PSE}}(\tau, t_w, \tau) \propto [C(\tau, t_w, \tau)A(t_w)]^2,$$

$$\begin{aligned}
C(\tau, t_w, \tau) &= \left\langle \left\langle \left\langle \exp \left[i \sum_j^N \left(\int_0^\tau \Delta \omega_j(t') dt' - \int_{t_w+\tau}^{t_w+2\tau} \Delta \omega_j(t') dt' \right) \right] \right\rangle \right\rangle \right\rangle \\
&= \left\langle \left\langle \left\langle \exp \left[i \sum_j^N \phi_j(\tau, t_w) \right] \right\rangle \right\rangle \right\rangle, \quad (1) \\
A(t_w) &= 2 \exp\left(-\frac{t_w}{T_1}\right) + \phi_{isc} \left[\exp(-k_{31}t_w) - \exp\left(\frac{t_w}{T_1}\right) \right].
\end{aligned}$$

The phase loss during the echo cycle is given by $\phi_j(\tau, t_w)$. Triple brackets indicate averaging over (1) the spatial distribution of TLS's; (2) the random history path of the TLS "spin flips"; and (3) the tunnel parameter λ and asymmetry Δ of the TLS's. The term $A(t_w)$ describes the loss of echo signal due to all population relaxation processes that occur within the waiting time t_w .⁴⁴ In a three-level system $A(t_w)$ contains the fluorescence life time T_1 , the life time of the triplet state $1/k_{31}$ and the intersystem crossing yield ϕ_{isc} .

The first average in the four-time correlation function that we have to deal with is the average over the spatial distribution of the perturbors in the glass. In order to do this some approximations have to be made. First, it is assumed that all TLS's and chromophores are distributed uniformly in space. Second, the interaction between the optical centre and the TLS's is assumed to be inversely proportional to the cube of the distance between chromophore and TLS, which corresponds to a dipolar coupling mechanism. It has been

shown^{45,46} that within this theory such a coupling is necessary to account for the observed exponential echo decays (Lorentzian linewidths) and is furthermore consistent with the observed temperature dependence of the optical dephasing time constant. At this point, however, nothing is claimed concerning the nature of the dipolar interaction. It can be due to either coupling of the electric dipole of a TLS to the permanent dipole in the chromophore's ground and excited state or, as is often assumed, elastic dipolar coupling. In the latter case the strain field at the position of the chromophore, which is caused by the elastic dipoles of the perturbors, couples to the electronic states of the chromophore. Furthermore, the effect of the reverse interaction of the excited chromophore on the TLS's is ignored and the interaction among the TLS's themselves is assumed to be very weak, so that the TLS's are statistically independent. The spatial average over all chromophore environments can now be executed, yielding^{26,28,29}

$$C(\tau, t_w, \tau) = \exp\langle -\Delta \omega_{1/2} \phi(\tau, t_w) \rangle_{H, \lambda, \Delta}. \quad (2)$$

In this expression $\Delta \omega_{1/2}$ is a constant that contains the chromophore-TLS dipolar coupling strength as well as the density of TLS's.

The second average in Eq. (1) that has to be dealt with is the summation over all possible history paths of the flipping TLS's. This average has been performed by Hu and Walker using a "sudden jump" model for the frequency fluctuations: $\Delta \omega(t) = h(t) \Delta \omega$, in which $h(t)$ is a random telegraph function that can take the values plus or minus 1 and changes sign whenever a TLS flips.²⁹ They find an expression for the inverse Laplace transform of the history average $\langle \phi(\tau, t_w) \rangle_H$

$$\begin{aligned}
&\int_0^\infty \langle \phi(\tau, t_w) \rangle_H \exp(-\sigma \tau) d\tau \\
&= \frac{1}{2} \operatorname{sech}^2\left(\frac{x}{2}\right) \frac{(2R/\sigma) + [1 - \exp(-Rt_w)]}{\sigma^2 \left[(1 + 2R/\sigma) \left(1 + \frac{2R}{\sigma[1 + \exp(x)]} \right) \left(1 + \frac{2R}{\sigma[1 + \exp(-x)]} \right) \right]^{1/2}} \quad (3)
\end{aligned}$$

with

$$x = \frac{E}{kT}$$

in which R , the total relaxation rate of a TLS, is equal to the sum of its upwards and downwards transition probabilities: $R = w_\uparrow + w_\downarrow$. Making use of the detailed balance condition: $w_\uparrow/w_\downarrow = \exp(-E/kT)$, the inverse Laplace transform of Eq. (3) can be performed which gives the result^{29,47}

$$\begin{aligned}
C(\tau, t_w, \tau) &= \exp[-\Delta \omega_{1/2} \langle F(R\tau) \\
&\quad + [1 - \exp(-Rt_w)] G(R\tau) \rangle_{\lambda, \Delta}] \quad (4)
\end{aligned}$$

where $F(R\tau)$ and $G(R\tau)$ are complicated integral functions.²⁹ At this point we are only left over with the average over the TLS parameters λ and Δ . Under the assump-

tions that the TLS's are weakly coupled to the phonon bath so that only one-phonon processes are important in the tunnelling process and that λ and Δ are uncorrelated, this average can be transformed into an average over the energy E and the relaxation rate R of a TLS.⁴⁸

For zero waiting time the stimulated photon echo becomes a two-pulse photon echo, which according to Eq. (4) is described by the function $F(R\tau)$. It can be shown that the function $F(R\tau)$ goes to zero for $R \gg 1/\tau$ and $R \ll 1/\tau$. As a consequence, only those perturbors which relax on the time scale of the measured optical dephasing process ($R \approx 1/\tau$) will contribute to the two pulse echo (2PE) decay. The exact shape of the 2PE decay is also determined by the distribution function of the internal TLS parameters. Maynard *et al.*⁴⁶ showed that in order to obtain an exponential 2PE decay, which is observed in many experiments, a hyperbolic distri-

bution function of relaxation rates is required: $P(R) \propto 1/R$.

The function $G(R\tau)$ in Eq. (4) becomes important for $t_w > 0$. Note that $G(R\tau)$ is only a function of τ and not of t_w . The term $G(R\tau)[1 - \exp(-Rt_w)]$ describes the additional dephasing that is caused by flipping of TLS's during the waiting time t_w . Slowly flipping TLS's which are static on the time scale of τ can make their contribution via this term. In the literature the name "spectral diffusion" is usually assigned to this "additional" dephasing process. It is, however, important to realize that a separation between "real" homogeneous dephasing (as measured in a 2PE) and spectral diffusion (as measured by 3PSE's) cannot be made. The 2PE decay is caused by exactly the same physical process that is responsible for spectral diffusion, namely flipping of TLS's. In both cases the optical transition frequency *diffuses* in frequency space due to flipping of TLS's, the only difference is the time/scale of the flipping process.

The function $G(R\tau)$ behaves different from $F(R\tau)$; together with the term $1 - \exp(-Rt_w)$ it forms a window function, which is constant between $1/\tau < R < 1/t_w$ and zero elsewhere. Measurement of the stimulated photon echo as a function of t_w therefore can be used to map out the distribution function of tunneling rates. Furthermore, it should be noted that $F(R\tau)$ and $G(R\tau)$ are intimately related: The 2PE decay strictly determines the amount of spectral diffusion that is observed for longer waiting times. Faster 2PE decays will result in more prominent spectral diffusion.

As the waiting time increases, the G term becomes the dominant part of the correlation function. In the limit that $R, 1/t_w \ll 1/\tau$ (or equivalently $R, 1/t_w \ll \sigma$), the correlation function reduces to⁴⁷

$$\begin{aligned} C(\tau, t_w, \tau) &= \exp[-\Delta \omega_{1/2} \tau \langle \text{sech}^2(E/2kT) \\ &\quad \times [1 - \exp(-Rt_w)] \rangle_{\lambda, \Delta}] \\ &= \exp[-k_{\text{corr}} \tau]. \end{aligned} \quad (5)$$

In this long-waiting-time limit the observed echo decay always has an exponential time dependence. This exponential behavior is independent of the form of the distribution of TLS parameters, but is solely due to the assumption of dipolar coupling to uniformly distributed and statistically independent TLS's.

The decay rate k_{corr} of the correlation function and its derivative can now be written as:

$$\begin{aligned} k_{\text{corr}} &= \frac{2}{T_2^* \text{eff}} \int_0^\infty dR P(R) [1 - \exp(-Rt_w)], \\ \frac{\partial k_{\text{corr}}}{\partial t_w} &\propto \int_0^\infty dR R P(R) \exp(-Rt_w) \end{aligned} \quad (6)$$

The second relation shows that for long waiting times the derivative of the echo decay rate with respect to t_w is directly proportional to the Laplace transform of R times $P(R)$. In the case that $R \cdot P(R)$ is a slowly varying function of R one derives:

$$\frac{\partial k_{\text{corr}}}{\partial \ln(t_w)} \propto P_I(1/t_w) \quad \text{with} \quad P_I(R) = R \cdot P(R) \quad (7)$$

So, if the echo decay time is measured for a series of waiting times and if subsequently the inverse time constants are plotted as a function of the logarithm of t_w , then the slope of this plot will be proportional to R times $P(R)$.

In deriving the correlation function it has been assumed so far that the distribution of the density of states of TLS's is constant over the energy range of interest: $P(R, E) = P(R)$. It can be shown that such a DOS leads to a linear temperature dependence of the homogeneous linewidth. However, in general a power law is observed in glasses: $(T_2^*)^{-1} \propto T^{1+\mu}$, with $\mu \approx 0.3$. This temperature dependence can be explained by relaxing the assumption of a constant DOS and letting $P(R, E) = P_0 E^\mu / R$. Support for this DOS is found in the temperature dependence of the specific heat of glasses.^{49,50} The correlation function [Eq. (2)] can, in the long-waiting-time limit, then be rewritten as

$$\begin{aligned} C(\tau, t_w, \tau) &= \exp \\ &\times \left[-\Delta \omega_{1/2} (kT)^{1+\mu} \tau \int_{R_{\min}}^{R_{\max}} dR \frac{1 - \exp(-Rt_w)}{R} \right. \\ &\quad \left. \times \int_{x_{\min}}^{x_{\max}} dx x^\mu \text{sech}^2(x/2) \right], \end{aligned}$$

where

$$x = \frac{E}{kT} \quad (8)$$

It should be noted that recently Jankowiak and Small⁵¹ claimed that the $T^{1+\mu}$ temperature dependence does not stem from $\rho(E)$ but is instead related to the average value of the TLS asymmetry parameter $\langle \Delta \rangle_E$. By using Gaussian distributions for λ and Δ they obtain a similar temperature dependence over a wide temperature range. Irrespective of the origin of the power law, we will use throughout this paper the expression for the four-time correlation function of Eq. (8), which is valid for both cases.

III. EXPERIMENT

The setup to detect photon echoes consists of two amplified synchronously pumped dye lasers (see Fig. 1). A setup with only one YAG laser would be sufficient for the detection of 2PE's and normal 3PSE's with waiting times of less than 15 ns. These waiting times can be obtained by increasing the optical path length of the third pulse up to several meters by use of an optical delay line. However, for longer waiting times the use of a second YAG laser is necessary. This laser can be delayed with respect to the first YAG laser in steps of the time interval between the argon pulses (12.2 ns). The delay can electronically be varied from zero up to hundreds of milliseconds.

The first YAG laser is used for amplification of the first and second excitation pulses in the 3PSE excitation sequence. The delay τ between these two pulses can be established with a translation stage (VD1), driven by a stepper motor. The second YAG laser is used for the amplification of the third excitation pulse. All three excitation pulses are derived from the same dye laser. The other dye laser is used for

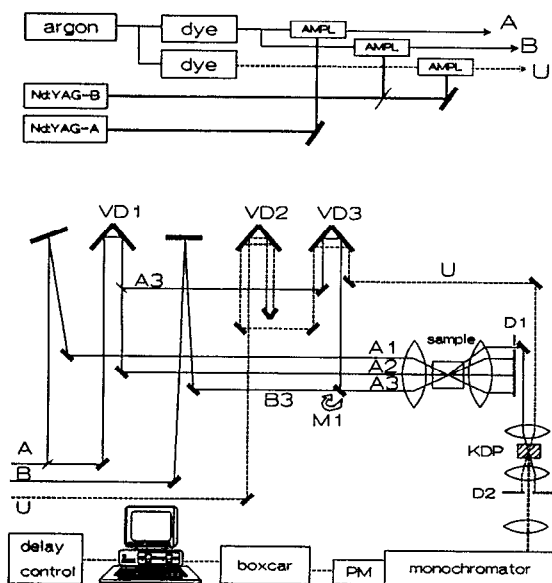


FIG. 1. The top part of the figure represents the amplified synchronously pumped dye laser setup that produces picosecond pulses. In the bottom part a layout of the beam paths near the sample is shown. Abbreviations: A1 and A2=first and second excitation beams, A3=third excitation beam used for regular photon echoes, B3=third excitation beam used for long-lived stimulated photon echoes, U=up-conversion beam, D=diaphragm, M1=rotatable mirror, PM=photomultiplier, KDP=frequency doubling crystal.

upconversion of the echo signal and is amplified by the second YAG laser as well. The trigger for this YAG also synchronizes the boxcar integrator, which detects the 3PSE signal.

An important aspect of this setup is that it allows for the detection of all echo's (2PE, 3PSE, long-lived 3PSE) coming from one and the same spot in the sample. To measure the 2PE both YAG lasers A and B fire at the same time. From the amplified excitation pulses only beam A is used, beam B is blocked. Beam A (amplified by YAG A) is split in two parts of which one travels through the variable delay VD1 and then is split again. Beam A3 is led through another delay VD3. Subsequently, the three beams are made parallel and focused with a lens ($f=160$ mm) in the sample. The angle between the beams is approximately 1.5° . Delay VD1 determines the time τ , which can be scanned from zero to 1.5 ns, controlled by a computer. With delay VD3 an independent control by hand of t_w is possible which can be varied from 0 to 13 ns. In order to achieve such long delays, a translation stage is needed with a length of at least 2 m.

The up-conversion pulse U has to be synchronized with the echo signal. The echo appears at time $t_w + 2\tau$. So if the time τ is scanned, U has to be delayed by 2τ . For that reason the probe beam (amplified by YAG B) is led twice through delay VD2 and once through VD3 before it is mixed with the echo signal in a KDP crystal.⁵² The translation stages VD1 and VD2 are run at the same speed.

In this way 2PE and 3PSE with $t_w < 13$ ns can be measured. If we want to extend the waiting time to longer times, all that has to be done is to swing away mirror M1. This results in blocking A3 and letting through B3 (amplified by

YAG B). Alignment of this part of the setup has to be done very carefully to assure that the optical paths of A3 and B3 are exactly the same. The delay t_w of both B3 and U can now electronically be controlled by establishing a delay between the firing of YAG A and B. The echo signal appears at time τ after the third pulse B3. Note that in this configuration the translation stage VD2 has to be driven at half the speed of VD1.

The chromophores zinc porphyrin (ZnP), magnesium porphyrin (MgP, both purchased from The Porphyrin Products) and meso-tetra-*p*-tolyl-zinc-tetrabenzoporphyrin (TZT, purchased from Syncom) were used without further purification. These metal porphyrins were chosen as probe molecules because of their high intersystem crossing yields and long triplet state lifetimes (about 100 ms). Pentacene (Fluka, used as supplied) has a much shorter triplet state lifetime (tens of microseconds). Deuterated ethanol (C_2H_5OD) and toluene were used as supplied (Janssen, p.A.). Deuterated ethanol was used to minimize the effect of hole burning during the photon echo measurements and no corrections for hole burning were found to be necessary. Triethylamine (Janssen) was distilled from KOH pellets prior to use.

A solution of the probe molecule in the glass-forming liquid was made with a concentration between $5 \times 10^{-4} - 1 \times 10^{-3}$ M. Part of this solution was transferred into a square cuvette ($10 \times 10 \times 1$ mm) attached to a vacuum line. The solution was carefully degassed by going four times through the cycle of cooling with liquid nitrogen, pumping and heating to room temperature again. Finally the cuvette was sealed under low pressure (10–100 Torr). Glasses were prepared by either putting the sample in a precooled cryostat at nitrogen temperature or plunging it directly into liquid helium.

Samples of chromophores in a polymeric matrix were obtained by pressing the doped polymer material, which was prepared by making a solution of the polymer [polystyrene (PS), polymethylmethacrylate (PMMA) or polyvinylbutyral (PVB), Janssen] and the chromophore in toluene or methylene chloride. The solvent was removed on a Rotavap and the rough material was dried overnight under vacuum. A small amount of this material was put in a template ($10 \times 10 \times 1$ mm) in a preheated ($200^\circ C$) hydraulic press. The polymer was heated during 3 min and degassed by increasing and releasing the pressure. Finally the pressure was increased to 50 kg/cm^2 during 2 min. The template was then cooled as fast as possible by flowing cold water through the pressing shoes. Hereafter the sample could be removed. Pentacene/PMMA had to be transferred very quickly to a precooled cryostat, or stored in an oxygen-free dark environment to prevent sample degradation.

IV. TEST OF THE SETUP ON A MOLECULAR MIXED CRYSTAL: PENTACENE IN NAPHTHALENE

In this section results of long-lived photon echo experiments on the molecular mixed crystal pentacene in naphthalene are presented. This presentation serves two purposes. First, it is meant to illustrate the possibility of making measurements in two different dimensions of the photon echo. Second, these echo measurements serve as a test of our ex-

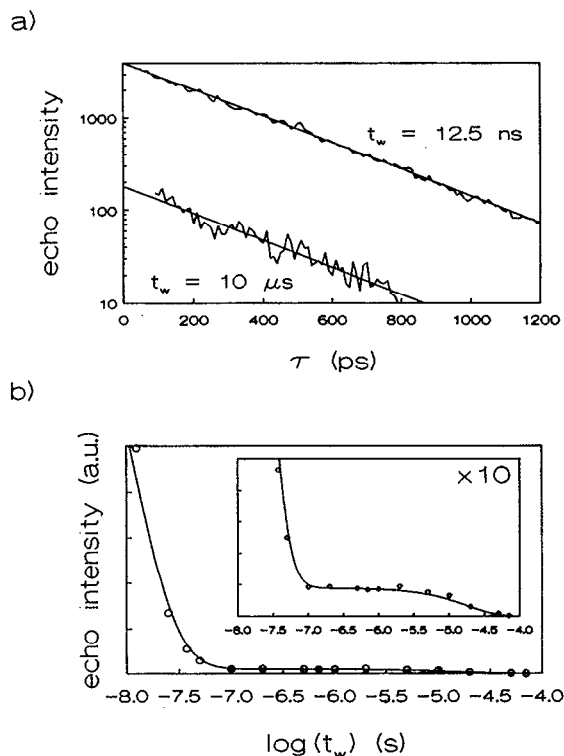


FIG. 2. Long-lived stimulated photon echoes in the molecular mixed crystal pentacene/naphthalene at 4.2 K. (a) Measurement in which the time τ between the first and second excitation pulses is varied and t_w , the time between the second and third pulses, is kept constant (coherence dimension). (b) Measurement where τ is constant and t_w is varied (population dimension).

perimental setup. Agreement with previous independent measurements on the same system exclude possible artefacts of the setup.

From extensive photon echo studies in the past⁵³ it is well known that a separation of time scales can be made in molecular mixed crystals like pentacene/naphthalene. The correlation function Eq. (2) then reduces to $C(\tau, t_w, \tau) = C(\tau) = \exp(-2\tau/T_2)$, where T_2 is the homogeneous dephasing time, and the optical Bloch equations completely describe the echo dynamics. The echo now provides the opportunity to determine independently the dephasing time T_2 and the population relaxation constants contained in $A(t_w)$ by, respectively, varying τ for a fixed t_w and varying t_w while keeping τ constant. We will refer to these two cases as the coherence dimension and the population dimension of the 3PSE.

Results obtained in the two dimensions of the photon echo on the system pentacene in naphthalene are depicted in Fig. 2. In Fig. 2(a) the logarithm of the 3PSE intensity is plotted for two different (fixed) waiting times t_w as a function of the time τ between the first and second excitation pulses. These are echo measurements in the coherence dimension and they yield the dephasing time T_2 . From the picture it can be seen that both echo decays for $t_w = 12.5$ ns and $t_w = 10$ μ s are single exponential and, more importantly, they both yield the same value for the echo decay time,

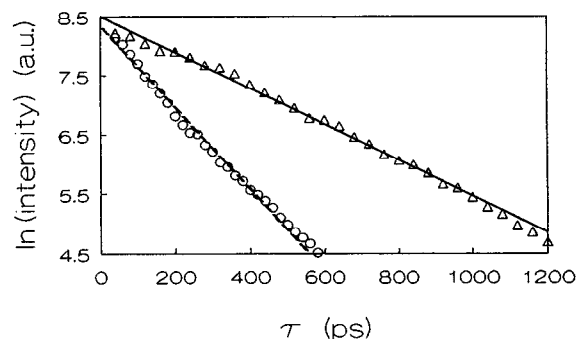


FIG. 3. Decays of a two pulse echo (triangles) and a long-lived stimulated photon echo (3PSE, circles) with a waiting time $t_w = 1$ μ s. The dashed line is a single exponential fit, the solid line is calculated from the distribution function obtained from a series of 3PSE measurements.

$T_2/4 = 300$ ps, in very good agreement with previous studies.⁵³ This is to be expected in the case where the optical Bloch equations apply: The dephasing time is independent of the waiting time of the measurement.

Figure 2(b) shows the result of the long-lived 3PSE experiment in the population dimension: The echo intensity is measured for a fixed pulse separation $\tau = 100$ ps as a function of (the logarithm of) the waiting time. The signal decreases rapidly with increasing t_w due to the relaxation of the excited state into the ground and the triplet states. The echo becomes long lived for waiting times longer than approximately 100 ns, only the ground state grating is then left over. The decay in the μ s region is caused by the limited lifetime of the triplet state. A fit to the experimental data using Eq. (2) yields values for the lifetimes ($T_1 = 20$ ns, $T_{\text{triplet}} \approx 35$ μ s) that agree well with the results of Hesselink.⁵³

V. RESULTS IN THE COHERENCE DIMENSION OF THE 3PSE

A. Glass dynamics of deuterated ethanol

In this section photon echo measurements on several porphyrins in deuterated ethanol will be presented. Part of the experiments on ZnP in EtOD have previously been published,⁴² but in order to enable a comparison with the other chromophores and to discuss possible distribution functions of fluctuation rates in detail, we have chosen to recapitulate these results.

Figure 3 displays two typical low-temperature photon echo decays in the system ZnP/EtOD. The triangles represent the 2PE, the circles are the 3PSE with a waiting time of 1 μ s, both on the same spot of the same sample at 1.5 K. Note that both echo decays are slightly nonexponential. While the 2PE decay tends to decay faster for longer delays, the 3PSE decay shows the opposite trend. The turn-over point is found for a waiting time of approximately 5 ns. The 3PSE behavior is consistent with the Hu and Walker theory and the deviation from exponential decay can be ascribed to the fact that the long-waiting-time limit is not yet completely reached. The function $F(R\tau)$ in Eq. (4) cannot completely be neglected with respect to $G(R\tau)$, since the 3PSE decay is at most only

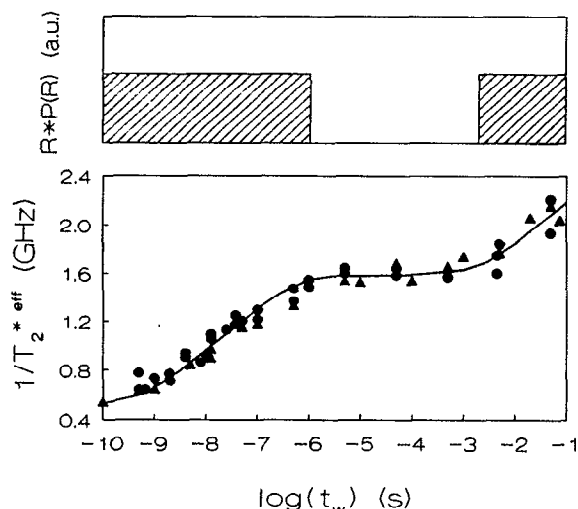


FIG. 4. Plot of the inverse of the effective pure dephasing time as function of the waiting time t_w of the echo experiment. The solid line is a fit to the data using the distribution function, which is pictured above. The circles and triangles refer to slowly and rapidly cooled samples, respectively (see the text).

a factor of 4–5 faster than the 2PE decay over the measured range of waiting times. The contribution of $F(R\tau)$ will relatively be more significant for larger τ , which leads to a somewhat slower echo decay with increasing τ . The nonexponentiality of the 2PE might indicate a slight deviation of a $1/R$ distribution function of relaxation rates in this glass for very short times. However, to a first approximation all echo decays can be fitted reasonably well by a single exponent and described within the long-waiting time limit for $t_w > 100$ ns. The following analysis is based on these assumptions.

The echo decay can be measured for many different waiting times and an effective dephasing time T_2^{eff} is obtained for each t_w by fitting the decay to an exponential function. The pure dephasing time $T_2^{*\text{eff}}$ is then calculated by removing the lifetime contribution according to $1/T_2^{*\text{eff}} = 1/T_2^{\text{eff}} - 1/(2T_1)$. The result is depicted in Fig. 4.

In this figure the inverse of the *effective* pure dephasing time, as measured in two series of 3PSE experiments, is given as a function of the logarithm of the waiting time t_w . In this plot it can be seen that for short waiting times the dephasing time decreases until it reaches a plateau at $t_w \approx 1$ μ s. The dephasing time remains constant up to the ms region where it continues its downward trend. The ensemble of TLS's that have an effect on the observed dephasing time is limited by the "window function" $[1 - \exp(-Rt_w)]$. This function allows only those TLS's that relax faster than $1/t_w$ to contribute to the measured value of $T_2^{*\text{eff}}$. Therefore, the presence of a plateau in Fig. 4 immediately signals a gap in the distribution function of the relaxation rates of TLS's $P(R)$: if TLS's with relaxation rates in this region would have been present then this would have resulted in faster echo decays.

More insight into the frequency dependence of $P(R)$ can be obtained by using Eq. (7), derived by Bai and Fayer⁴⁷ for the long waiting time limit. This relation states that the slope

of the plot in Fig. 4 is, in the case of a slowly varying distribution function, proportional to $P_1(1/t_w)$ with $P_1(R) = R \cdot P(R)$. A constant slope will thus yield a hyperbolic distribution of relaxation rates: $P(R) \propto 1/R$. This functional form of $P(R)$ is, within the stochastic sudden-jump model, also a requirement for single exponential 2PE decays. A hyperbolic distribution of relaxation rates therefore seems to be a reasonable start in the fitting procedure. The data can then be fit to

$$\frac{1}{T_2^{*\text{eff}}(t_w)} = \frac{1}{T_2^{*\text{eff}}(1/R_{\text{max}})} + \frac{1}{2} \int_{R_{\text{min}}}^{R_{\text{max}}} dR P(R) \times [1 - \exp(-Rt_w)] \quad (9)$$

with

$$P(R) = \frac{\omega}{R}.$$

The condition $1/t_w < R_{\text{max}} < 1/(10\tau)$ should be fulfilled to remain in the long waiting time limit. The factor 1/2 arises from the fact that the decay rate of the correlation function is equal to $2/T_2^{*\text{eff}}$.

If the waiting time becomes on the order of the dephasing time then the approximation of Bai and Fayer is no longer valid and the exact Hu and Walker Eq. (3) has to be used instead. The distribution function $P(R)$ has to be inserted into this expression and the integral can be evaluated numerically. The inverse Laplace transformation can be performed using the Stehfest algorithm.^{23,54} The correlation function is then given by the exponential of the inverse Laplace transform multiplied by minus one. The echo decay function can be calculated for any waiting time following this procedure. By fitting the decay to a single exponential function the pure dephasing time is obtained.

Using the combination of the long waiting time equations and the exact expression, we were able to make an excellent fit to the data as indicated by the solid line in Fig. 4. The fit was made with a distribution function of the following form:

$$P(R) = \begin{cases} \omega/R & \log R > 6 \text{ and } \log R < 2.5 \\ 0 & 2.5 < \log R < 6 \end{cases}, \quad (10)$$

where $\omega = 280$ MHz. This distribution is depicted as the shaded area in Fig. 4.

With this choice of $P(R)$ the 2PE decay can be calculated as well.⁵⁵ The decay constant T_2 of the 2PE is given by the relation

$$\frac{1}{T_2^{\text{2PE}}} = \frac{\theta\omega}{2} + \frac{1}{2T_1}. \quad (11)$$

Here, θ is a numerical constant equal to 3.66⁴⁶ and T_1 is the population relaxation time of the excited state. The solid line in Fig. 3 represents the calculated 2PE decay, which agrees very well with the experimentally observed decay. Although this may seem to be almost trivial, it stresses the point that the amount of spectral diffusion during t_w is completely determined by the value of the decay constant of the 2PE decay. A relationship between the functions $F(R\tau)$ and $G(R\tau)$

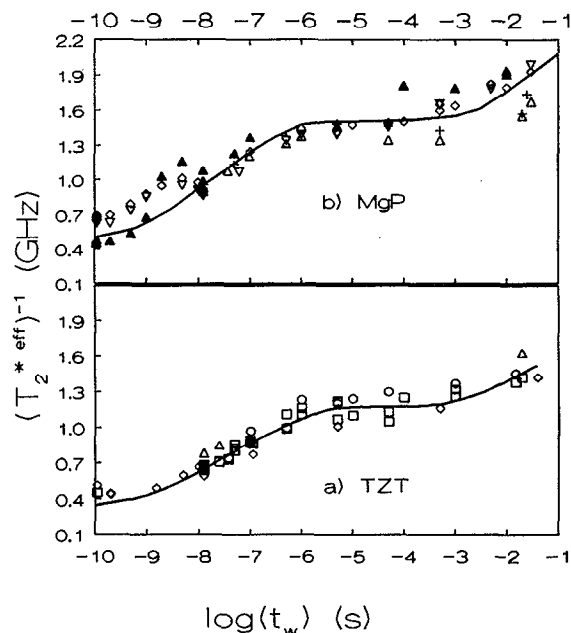


FIG. 5. The inverse effective pure dephasing time as a function of the waiting time t_w for magnesiumporphyrin (MgP) and meso-tetra-*p*-tolyl-zinc-tetrabenzoporphyrin (TZT) in deuterated ethanol (C_2H_5OD). The fits have been made using a hyperbolic distribution function $P(R) = \omega/R$, where $\omega = 270$ MHz and $\omega = 160$ MHz, respectively.

[Eq. (4)] exists: a faster 2PE decay will also be reflected in more spectral diffusion in the 3PSE decays. The conclusion therefore is that all photon echo data with waiting times less than $1 \mu s$ can be self-consistently described using a single hyperbolic distribution function of relaxation rates. For longer waiting times the existence of a gap in $P(R)$ has to be invoked.

At this point it is important, however, to keep in mind that a hyperbolic distribution function is a plausible but not necessarily the true distribution function. Any subtle structure in the real distribution function will be smoothed by integration over the window function $\{1 - \exp(-Rt_w)\}$. The rising edge of this window function therefore puts a severe restriction on the achievable resolution of details in the distribution function. As will be shown below, it is quite possible to make an acceptable fit to our data using different distribution functions. However, in order to yield an exponential decay of the 2PE, these functions should not deviate too much from a hyperbolic one in the short-waiting time limit. Despite the limitations of the inverse Laplace transform analysis, and regardless of what functional form for the distribution function is used, a clear minimum or gap in the μs -ms region of the distribution function is needed to describe our data.

Before coming to a discussion of this gap in $P(R)$ some measurements with different probes in an EtOD glass will be presented. In Fig. 5 the inverse pure dephasing time is plotted as a function of t_w for the metal porphyrins TZT and MgP. The fits are made using the functional dependence of $P(R)$ with a gap between $1 \mu s$ and $3 ms$ as in Eq. (10), only the coupling constant ω is used as a fitting parameter. It is clear

from this figure that the observed shape of the distribution function is independent of the probe molecule. The only differences are contained in the parameter ω which is varied to allow for a different coupling strength of the TLS's to the optical probe. The value of ω is slightly lower in case of the TZT probe, and, as a consequence, the amount of spectral diffusion is slightly less in this system. The MgP data can be fitted with almost the same value of ω as ZnP, although the scatter in the data is much larger due to very weak echo signals in MgP/EtOD. Note that this result is different from hole burning measurements on milliseconds-seconds timescale performed by Van der Zaag *et al.*⁵⁶ on porphyrins in (polycrystalline) polyethylene (PE). They found a linear relationship between the effective pure dephasing time and the fluorescence lifetime of the probe molecule, which is not yet understood. For instance, the hole widths they find for MgP are much narrower than for ZnP, which has a much shorter fluorescence lifetime than MgP. The fact that using ZnP or MgP as a probe molecule in our 3PSE study makes no difference, shows that this (unexplained) relationship between T_2^{eff} and T_1 does not hold in an ethanol glass on timescales shorter than 100 ms. Its validity on longer time scales remains to be tested for different glasses.

The $1/R$ distribution function complies with our expectations based on the ubiquitous presence of $1/f$ noise in many solids,⁵⁷ but the existence of a gap in the glass dynamics that stretches from about 1 kHz to 1 MHz is most surprising. Obviously the glass structure prohibits the formation of tunneling centres whose dynamics would otherwise fall in the gap region. The stiffness in this frequency range could possibly be caused by the formation of a network in the glass by hydrogen bonding. It should be noted that transient hole burning measurements by the Fayer group^{22,55} revealed no such a gap between 1 and 100 kHz in a phase I ethanol glass. In previous papers^{42,58} we tentatively attributed the gap to the special type of order that is present in a phase II ethanol glass. Because at that time we could cool our samples only rather slowly, we assumed to perform measurements in the regime of the glassy plastic ethanol (phase II).⁵⁹ However, with the arrival of a new (bath) cryostat in our lab we were able to cool the samples more quickly by plunging the samples directly into liquid helium. In this way the samples could be cooled down to 4.2 K within ten seconds. Under these conditions the real amorphous phase I is supposed to be formed. The triangles in Fig. 4 represent measurements on such a very rapidly cooled sample (>20 K/s) while the circles have been acquired with a slowly cooled sample (<0.5 K/s). The dephasing times were found not to be related to the cooling rate. The small differences that were observed were on average comparable to differences, about 10%, obtained by measurements on different spots in one sample. Even after annealing above the glass transition temperature and subsequently cooling very slowly to 1.5 K the dephasing rates remained the same. Based on the result of PHB measurements by Van den Berg and Völker,³³ who found an order of magnitude slower dephasing in the phase II glass compared to phase I on minutes time scale, one would have expected different dephasing behavior as well. We conclude that we have either been unable to form the

phase II glass or that this phase shows the same dynamics as phase I of ethanol on time scales up to 100 ms. In both cases the hypothesis that the gap is related to the specific order in phase II ethanol has to be abandoned.

An explanation for the two seemingly contradicting observations concerning the gap might be found in the difference between the probe molecules. Littau and Fayer^{22,55} made use of the ionic dye cresylviolet. It seems plausible (as suggested by Fayer⁶⁰) that cresylviolet and a metal porphyrin have different mechanisms to couple to the TLS's in the glass. The neutral porphyrin chromophore does not possess a permanent electric dipole moment and can only interact with the glass via elastic dipole coupling, while the charged ionic cresylviolet permits electric dipole coupling as well. It may well be that the different probe molecules are therefore sensitive to different subsets of the complete TLS ensemble, which may have different distributions of fluctuation rates as well. However, it cannot be excluded yet that the gap is caused by the metal porphyrin itself. Since it is known that complexation of metal porphyrins in ethanol occurs, it is conceivable that the porphyrin induces a certain orientation of the ethanol molecules in its environment which could lead to dynamics which are different from the bulk glass dynamics. Additional stimulated photon echo experiments on different probe molecules in an ethanol glass are needed to come to a definite conclusion concerning the physics behind the gap in $P(R)$.

Recently, Jankowiak and Small⁶¹ (J&S) published an alternative fit to our 3PSE data (and those of Littau and Fayer⁵⁵) using a different distribution function in both the weak and strong coupling limit. This function is based on the assumption that the distribution of the TLS-asymmetry parameter Δ and tunnel parameter λ can be represented by Gaussian functions and that Δ and λ are uncorrelated.⁶² In the weak coupling limit this results in a log-normal distribution for $P(R)$, in the case of strong coupling a similar function is obtained, which shows, however, pronounced tailing towards slower relaxation rates. They fitted our data to two log-normal distributions in the weak coupling case or to one distribution under strong coupling conditions. However, for this last fit they had to discard some of our data points and further assumed that the "apparent" gap is unreal. A few remarks concerning their analysis have to be made. First, the various measurements on ZnP and other probes in ethanol, together with echo experiments in the "population dimension" (see below) confirm the existence of a gap. Second, the sudden cutoffs in our distribution function are, of course, not physically realistic, but represent a first-order approximation to this function. The signal-to-noise ratio is not sufficient to determine the actual shape of the distribution function more accurately.

Given this state of affairs it is well possible, as Jankowiak and Small demonstrate, to make a fit using a log-normal distribution in the long-waiting time limit. The exponential decay of the echo is independent of the shape of the distribution function as long as the distribution function is slowly varying with respect to the logarithm of t_w . However, in the short-waiting time limit (the limit of the 2PE and 3PSE with short waiting times) the functional form of the echo decay is

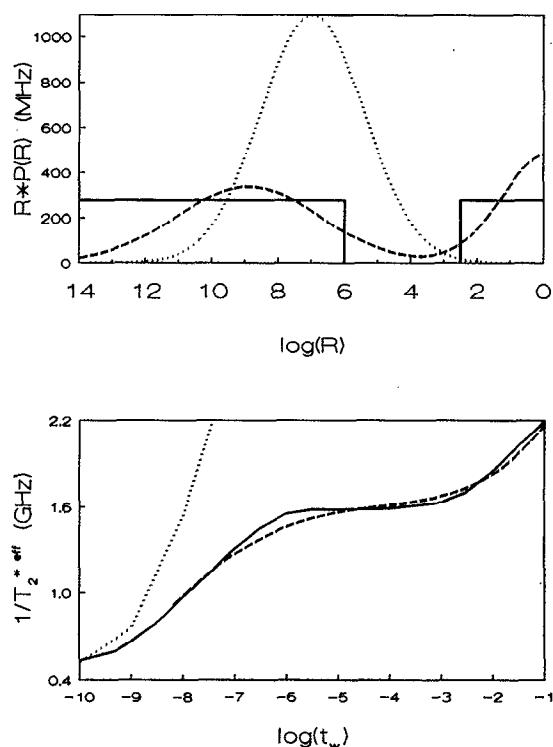


FIG. 6. The lower part of the figure shows the calculated dependence of the effective pure dephasing time on the waiting time of the echo experiment. Three different distribution function are used, one hyperbolic distribution function ($P(R) = \Omega/R$) and two log-normal distribution functions ($P(R) = (\Omega_0/R) \exp\{-[\ln(R/R_0)]^2/(2\sigma_0^2)\}$). These functions are depicted in the upper figure. Solid line: Hyperbolic distribution with $\Omega = 280$ MHz. Dotted line: Log-normal with $\log(R_0) = 6.97$, $\sigma_0 = 3.6$, and $\Omega_0 = 1100$ MHz (Jankowiak and Small, Ref. 61). Dashed line: Sum of two log-normals with $\log(R_0) = 8.9$, $\sigma_0 = 5$, $\Omega_0 = 340$ MHz and $\log(R_1) = -0.14$, $\sigma_1 = 3.21$, and $\Omega_1 = 486$ MHz.

intimately determined by the shape of the distribution function of relaxation rates. In this limit it is not correct, as Jankowiak and Small did, to make a distinction between spectral diffusion and pure dephasing. In fact, they subtract what they call the pure dephasing contribution (the homogeneous linewidth obtained from the 2PE) from the complete data set and assign the remaining relaxation effect to spectral diffusion. As both pure dephasing and spectral diffusion in glasses are caused by the same physical process, namely, TLS flipping, this approach is incorrect. For instance, the distribution function they derive goes to zero for $t_w \approx 1$ ps and therefore cannot account for the observed 2PE decay. A proper distribution function of relaxation rates, however, must also be capable of describing the exponential 2PE decay.

We have attempted to fit our data with a log-normal distribution. In Fig. 6 this distribution is compared with the previously used $1/R$ distribution and the J&S log-normal distribution. In order to yield a reasonable 2PE decay, the prefactor of the J&S function must be fairly high compared to the other functions. As a consequence, the slope of the $1/T_2^*$ curve is far too steep. Furthermore, such a distribution function yields a highly nonexponential 2PE decay, as can be observed in Fig. 7. The 2PE decay, which is obtained with

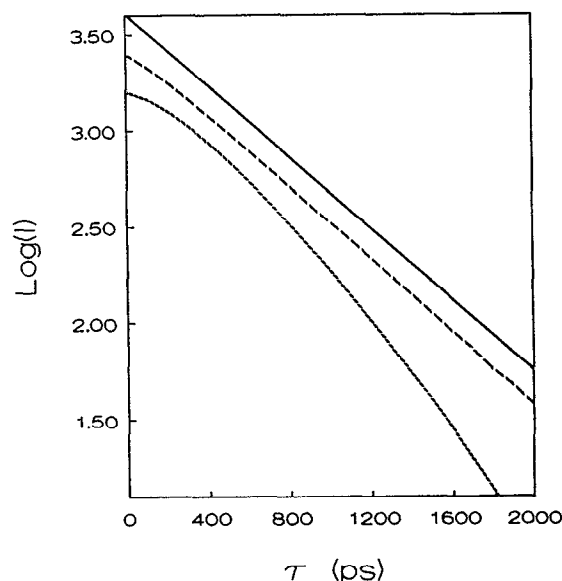


FIG. 7. Logarithmic plot of the calculated two pulse echo decay for two different log-normal distributions and a hyperbolic distribution function. The solid line is calculated using a hyperbolic distribution, the dotted line stems from the hyperbolic distribution function used by Jankowiak and Small (Ref. 61) and the dashed line is calculated with the sum of two log-normal distribution functions. The solid, dotted and dashed lines refer to the distribution functions as used in Fig. 6. The echo decays are arbitrarily shifted with respect to each other to facilitate comparison.

our log-normal distribution, is slightly nonexponential and reflects the observed experimental decay. From the figure it can be seen that the deviation from a $1/R$ distribution in the 2PE region [$\log(R) = 12-9$] is only a factor of 2, while the J&S function changes by about 2 orders of magnitude. Therefore, we conclude that a log-normal distribution can only describe the 2PE decay as long as its functional form does not differ too much from a hyperbolic distribution in the 2PE region. Since it is not yet possible to extract accurately the shape of the distribution function from the experimental data, we will use throughout the rest of this paper hyperbolic distribution functions as the basis of our fits.

Finally, we want to remark that our echo measurements are not the only experiments that reveal a gap in the optical dynamics of an amorphous solid. Fleury *et al.*⁶³ recently presented data on the dynamics of perylene doped into polyethylene. By single-molecule fluorescence detection they were able to follow the frequency jumps of a single oscillator. By measuring the correlation function of the fluorescence they determined the relaxation times of the (few) TLS's to which this single molecule was coupled. A plot of the number of TLS's as a function of their characteristic relaxation time, measured from 1 μ s to approximately 10 s, showed two Gaussian-like distributions with a prominent dip in between at about a relaxation time of 1 ms.

B. The temperature dependence of optical dephasing

In this section we discuss the temperature dependence of the effective dephasing time. Figure 8 shows the result for

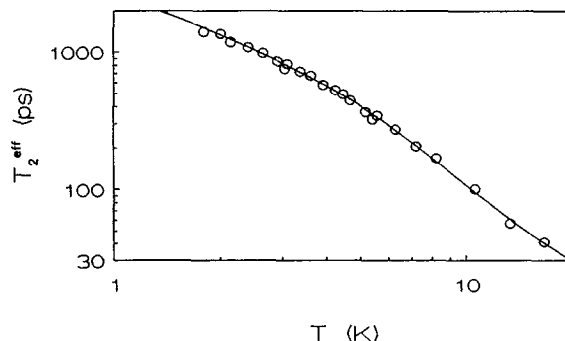


FIG. 8. The temperature dependence of the pure dephasing time in the system zincporphyrin in deuterated ethanol (C_2H_5OD) as measured in two pulse photon echo measurements. A fit to the data has been made using Eq. (12) with the parameters: $\alpha = 1.4 \pm 0.1$, $1/a = 4.6$ ns, $1/b = 16.2$ ps, $\Delta E = 21 \pm 4$ cm^{-1} , and $T_1 = 2.7$ ns.

the 2PE decay of ZnP in deuterated ethanol, plotted on a double logarithmic scale. A fit to the data has been made with the well known expression⁶⁴

$$\frac{1}{T_2} = \frac{1}{2T_1} + aT^\alpha + b \frac{\exp(-\Delta E/kT)}{1 - \exp(-\Delta E/kT)}. \quad (12)$$

The best fit yields the values $\alpha = 1.4 \pm 0.1$ and $\Delta E = 21 \pm 4$ cm^{-1} .

The last two terms describe pure dephasing which is caused by two different mechanisms. At very low temperatures the T^α term is dominant. This term is characteristic for TLS-induced dephasing in amorphous solids. All optical phonon contributions are frozen out and only tunneling centers contribute to dephasing. A power law T^α with $1 \leq \alpha \leq 2$ is generally observed. In many organic glasses α takes the value of approximately 1.3.⁶⁵ The same temperature dependence is also observed for the heat capacity.⁵⁰ This power law has been explained by conjecturing that the distribution of TLS energy splittings $P(E)$ is proportional to $E^{0.3}$.

At elevated temperatures the data start to deviate from a power law. Jackson and Silbey⁶⁴ proposed that at these temperatures another dephasing mechanism sets in, which can be modelled by an exponentially activated process. In molecular mixed crystals pseudolocalized librational motions of the guest chromophore in the host matrix cause such an activation. In glasses, however, the activation energy is independent of the chromophore but is strongly correlated to the host. The activation energy of 21 cm^{-1} we find is identical to the one obtained from photon echo experiments on rhodamine B and resorufin in a deuterated ethanol glass.⁶⁶ Since the structures of rhodamine B, resorufin and ZnP are very different, the exponentially activated dephasing process must be due to a mode of the glass itself. The fact that the data can be described using a single activation energy is consistent with coupling to a narrow-band optical mode of the host.^{66,67} Unfortunately, to our knowledge no exact identification of this host mode has yet been made in an ethanol glass.

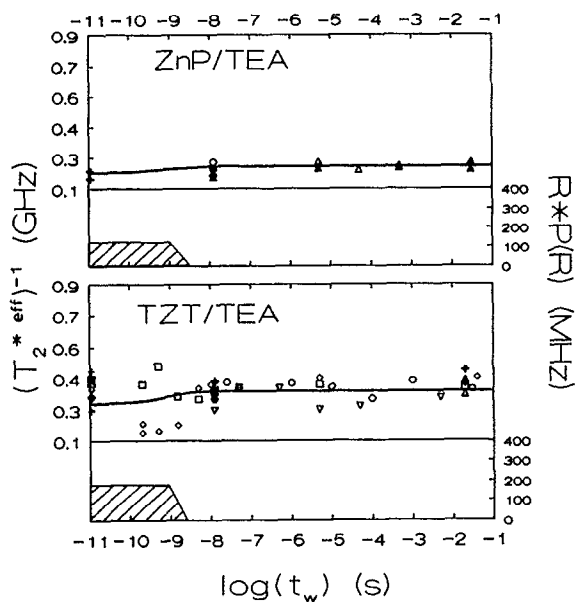


FIG. 9. Plots of the waiting time dependence of the effective pure dephasing time in triethylamine (TEA) glass at 1.5 K, using two different probe molecules: zincporphyrin (ZnP) and meso-tetra-*p*-tolyl-zinc-tetrabenzoporphyrin (TZT). Each symbol represents a series of measurements in one spot of the sample. The distribution functions, which are used to make the fit, are depicted as the shaded area.

C. Triethylamine: Only fast tunnel dynamics

In Fig. 9 the effective pure dephasing times for ZnP and TZT in TEA are plotted versus the logarithm of the waiting time. The results obtained for both chromophores look very similar: The effective pure dephasing times remain unchanged over the whole range of waiting times. This behavior accords with hole burning measurements by Wannemacher *et al.*,⁶⁸ who concluded, from a comparison of permanent and transient holewidths in the 0–0 transition of bacteriochlorophyll *a* in TEA, that at least over the range from 15 μ s to 100 s no spectral diffusion occurred in this glass. The observations together indicate that in TEA no TLS's exist with fluctuation rates in the region of 1 GHz to 0.01 Hz.

The low-temperature 2PE decay, however, is far from lifetime limited as T_2 is less than twice the fluorescence lifetime T_1 ($T_2 = 2.9$ ns $< 2T_1 = 7.4$ ns for ZnP in TEA). The only process that can be responsible for this effect at such low temperatures (1.5 K) in this glass is the tunneling of the TLS's. In order to account for the observed single exponential 2PE decay in the TLS model we have to assume that $R \cdot P(R)$ has a constant value in the region where R is on the order of $1/\tau$ and goes to zero for $R < 1/T_2$. Starting with such a distribution function (plotted in Fig. 9 as well) the echo decays were calculated using Eq. (3) and subsequently fitted with a single exponential function. The calculated pure dephasing times were adjusted to the experimental data by varying the coupling parameter ω and the cutoff rate for slowly relaxing TLS's.

The fall off of $P(R)$ at ~ 1 GHz will reflect itself in a nonexponential decay of the 2PE for large pulse separations

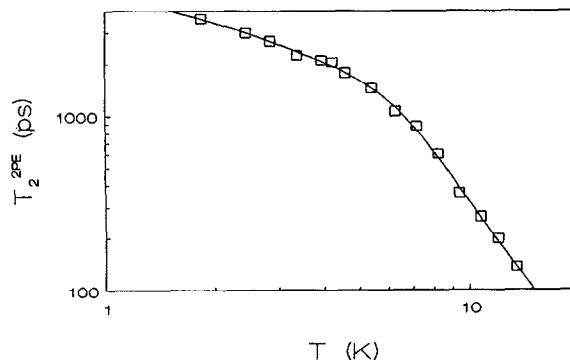


FIG. 10. The temperature dependence of the effective pure dephasing time in a triethylamine glass doped with zincporphyrin as measured in a 2PE experiment. The fit to the data has been calculated using Eq. (12) with the following parameters: $\alpha = 1.2 \pm 0.1$, $1/a = 1.4$ ns, $1/b = 8.3$ ps, $\Delta E = 29 \pm 3$ cm⁻¹, and $T_1 = 3.7$ ns.

τ (> 2 –5 ns). However, the maximum obtainable value for τ in our experiments was only 1.5 ns due to the limited length of the optical delay line. The calculated 2PE signal over this range deviates only slightly from exponential decay and given the signal-to-noise ratio of our setup it is unlikely that this deviation will be detectable.

The proposal that the 2PE dephasing at 1.5 K in TEA is caused by an ensemble of TLS's that relax within several ns is also supported by the temperature dependence of the 2PE decay. A double logarithmic plot of the homogeneous dephasing time as a function of the temperature is presented in Fig. 10. The slope of the curve shows a pronounced curvature between 5 and 6 K. As in other glasses the low temperature part ($T < 5$ K) can be very well described by a power law T^α with $\alpha = 1.2 \pm 0.1$, while at higher temperatures an exponentially activated process sets in. As already discussed earlier, the power law is characteristic for TLS induced dephasing and observed in many amorphous systems. We therefore conclude that the pure dephasing process as derived from the 2PE decay in TEA is mainly caused by an ensemble of fast relaxing TLS's. Apparently the TEA glass is ordered to the extent that fast (small) fluctuations can freely occur, but that larger structural rearrangements on slower time scales are prohibited.

At higher temperatures the dephasing is predominantly caused by a low frequency phonon of the TEA glass. The activation energy of this mode is approximately 29 cm⁻¹. Hole burning measurements on bacteriochlorophyll *a* in TEA⁶⁹ yield an activation energy on the order of 30 cm⁻¹ as well, which is in agreement with the idea that indeed a host mode is responsible.

D. Comparison between some organic glasses and polymers

We have performed waiting time dependent 3PSE studies in three organic glasses and two polymers as shown in Figs. 11(a) and 11(b). In all matrices the metal porphyrin TZT

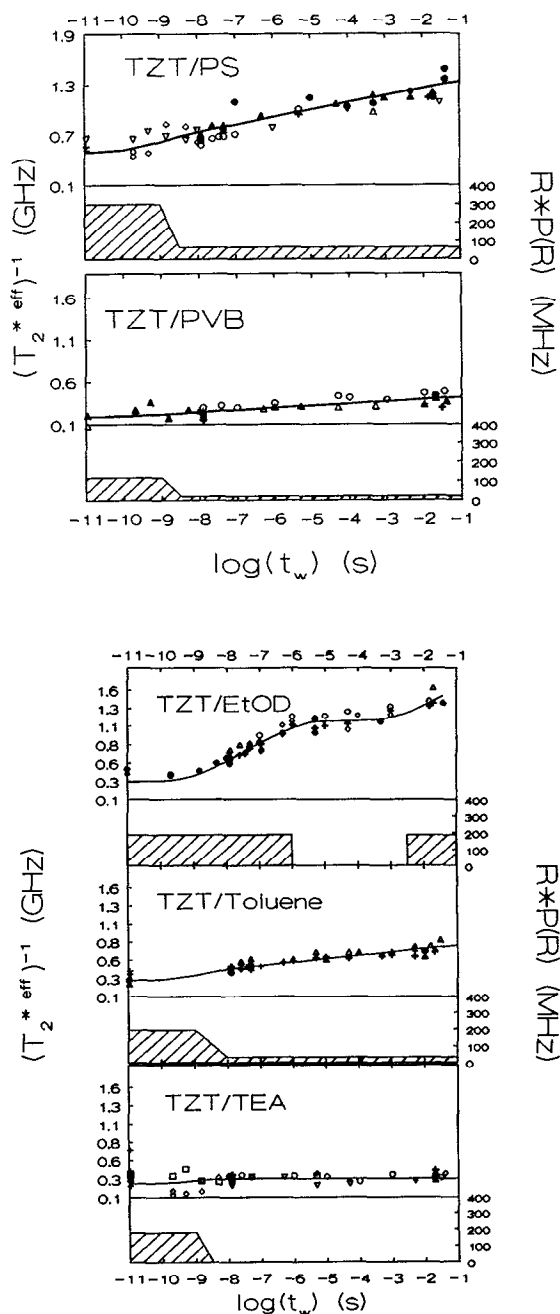


FIG. 11. (a) Comparison between the amount of spectral diffusion in the polymers polystyrene (PS) and polyvinylbutyral (PVB) using meso-tetra-*p*-tolyl-zinc-tetrabenzoporphin (TZT) as probe molecule. All measurements have been performed at 1.5 K. The different symbols indicate measurements on different spots of the sample. The distribution functions of fluctuation rates that have been used to make a fit to the data are indicated by the shaded area. (b) Spectral diffusion at 1.5 K in the organic glasses deuterated ethanol (C_2H_5OD), toluene and triethylamine (TEA) doped with meso-tetra-*p*-tolyl-zinc-tetrabenzoporphin (TZT).

was used as probe molecule. The various plots are drawn on the same scale to facilitate comparison between the different cases.

From this figure it is clear that the amount of spectral diffusion occurring between nanoseconds and milliseconds is

quite different in these systems. Ethanol shows the most pronounced spectral diffusion effect and is closely followed by polystyrene. Toluene reveals less time-dependent line broadening and in PVB this effect can only just be observed. In the system TZT/TEA the dephasing time does not change at all in the ns–ms time span. Spectral diffusion and the distribution function of fluctuation rates are obviously highly related to the specific structure of the host material and cannot be viewed as general properties that all glasses have in common.

The second salient feature in Fig. 11 is the fact that in none of the host materials the effective dephasing can be described by a single hyperbolic distribution function of relaxation rates from picoseconds to 100 ms. In all systems except ethanol, the amount of spectral diffusion is less than one would expect based on the value of the pure dephasing time measured by the 2PE. Therefore, somewhere between 1 GHz and 1 MHz the distribution function has to change dramatically. The distribution functions that have been used to make a fit to the experimental data are also presented in Fig. 11. The fitting procedure was the same as in the previous section: The value of ω for short waiting times can be extracted from the 2PE decay. The exact Eq. (3) is then used to calculate the echo decay for longer waiting times. However, since this value of ω would lead to too much spectral diffusion, a cutoff rate R_c , at which a crossover to another value of ω occurs, has been introduced. Both R_c and ω have been varied to obtain the best fit to the data. It turns out that the dynamics in these systems can very well be described by invoking two different hyperbolic distribution functions. One of them governs the fast relaxation region, causing the 2PE decay and the short waiting time spectral diffusion, while the other is responsible for the slower dynamics. In the case of ethanol the two distributions do not overlap and in TEA the second distribution is completely absent. One should keep in mind that the sudden changes in $P(R)$ as displayed in the figure are first order approximations and do not represent real physical behavior. Unfortunately, the experimental spread in our data is too large to determine the precise functional form of these changes.

It might well be possible that the two distribution functions are related to existence of intrinsic and extrinsic TLS's.^{32,61} In that case the fast fluctuation would be caused by the "sea" of distant glass TLS's, while the slower distribution function would be associated with changes involving the chromophore itself. Such a hypothesis could, in principle, be tested by comparing, for instance, deuterated with normal ethanol as host material. It is known that deuteration decreases the (nonphotochemical) hole burning efficiency by a factor of 30 but does not affect the homogeneous dephasing time. Since the external TLS_{ext} are generally held responsible for the occurrence of NPHB, one would expect a very different slow distribution function in case of normal ethanol. However, efficient hole burning deteriorates the photo/echo signal and therefore we have not yet been able to perform these kind of measurements.

E. Pentacene in polymethylmetacrylate revisited

About a decade ago Molenkamp and Wiersma⁷⁰ (M&W) reported on the dynamics of pentacene doped into polymethylmetacrylate (PMMA) using accumulated photon echoes and hole burning. Van den Berg and Völker³³ (B&V), however, reported a narrower hole width than was inferred from the accumulated photon echo decay obtained by M&W. Fidler *et al.*¹⁶ suspected that the cause of this discrepancy might be due to heating of the polymer in the echo experiments. This hypothesis was verified in a careful power- and temperature-dependent APE study in which very low excitation energies were used. After a temperature correction was made to account for the heating effects, the homogeneous linewidths were found to be narrower than obtained by hole burning (PHB). Unfortunately, at the time, a 2PE signal could not be detected in pentacene/PMMA, despite the fact that the strong APE signals could easily be obtained. The reason for this failure was sought in the presence of strong electron-phonon coupling in the pentacene-polymer system. Detection of APE signals was thought to be possible due to the higher sensitivity of this technique.

Motivated by the improved performance of our setup, we decided to make another attempt to measure 2PE's and 3PSE's in pentacene-doped PMMA. To optimize our chances of detecting an echo signal we made use of a three beam configuration for excitation of the 2PE to achieve perfect phase matching.⁷¹ Somewhat to our surprise this time the photon echo was easily found. It turned out, however, that both the echo decay time and the echo intensity were rather dependent on the energy of the excitation pulses. High pulse energies led to faster echo decays and weaker echo signals. The signal disappears completely if the total energy of all excitation pulses becomes on the order of 1 μ J. This effect is most likely the cause of our failure previously to measure the 2PE, since at that time higher pulse energies had to be used because of the lower detection sensitivity and because of imperfect phase matching in the 2PE.

The dephasing time was found to converge to a constant for pulse energies less than 20–30 nJ; higher pulse energies were found to accelerate the echo decay considerably. Although this behavior looks analogous to what was found in case of the APE,¹⁶ it cannot be explained by steady state heating of the polymer sample, because the dephasing time does not change upon an increase of the repetition rate and is therefore independent on the average fluence. We suggest that the observed power dependence of the echo decay is due to the multilevel nature of the pentacene system, in which a second photon excites the system to a higher excited state thereby depleting the echo signal. At the same time the ultrafast relaxation from this state dumps heat into the local lattice which leads to an instantaneous faster echo decay. Therefore, all measurements presented in this section were performed with total pulse energies of about 20 nJ and are in the region where the echo decay is no longer affected by this power effect.

The result of a waiting-time-dependent photon echo study at 1.7 K is depicted in Fig. 12 together with the corresponding distribution $R \cdot P(R)$. The increase of the inverse pure dephasing time with waiting time can consistently be

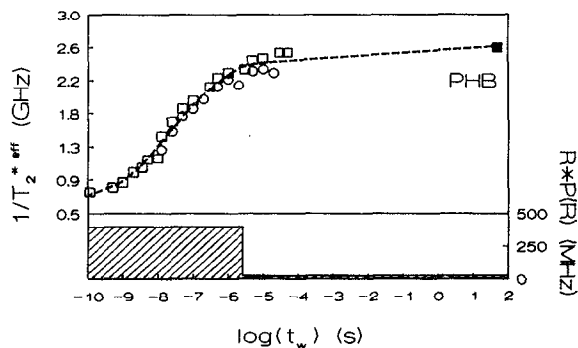


FIG. 12. Spectral diffusion at 1.7 K in polymethylmethacrylate doped with pentacene. The open squares and circles represent two series of measurements on two different spots in the sample. The solid square is derived from a persistent hole burning experiment and has been taken from Ref. 33. The distribution function that has been used to calculate the fit (dashed line) is pictured as the shaded area.

described up to 1–10 μ s by one hyperbolic distribution function. It is evident from the plot that for longer waiting times a significant deviation from logarithmic broadening sets in. Unfortunately this is also the region where the bottleneck expires and, as a consequence, not enough data points are available to determine the distribution function of the slower fluctuations with high accuracy. Nevertheless, the extrapolation that is made to the inverse pure dephasing time as measured by PHB³³ on the time scale of minutes seems to be justifiable. And again, as for other systems discussed in the previous section, the dynamics in this polymer also seems to be governed by two distribution functions.

To complete the pentacene-in-PMMA case, the temperature dependence of the homogeneous dephasing time was measured and the results are presented in Fig. 13. Using the combination of a power law and an exponential activation, a very good fit to the data could be achieved. The values for α and ΔE of 1.3 ± 0.1 and 15 ± 3 cm^{-1} , respectively, are very close to the ones ($\alpha = 1.3$ and $\Delta E = 14$ cm^{-1}) derived from APE measurements.¹⁶ It should be noted that the same value

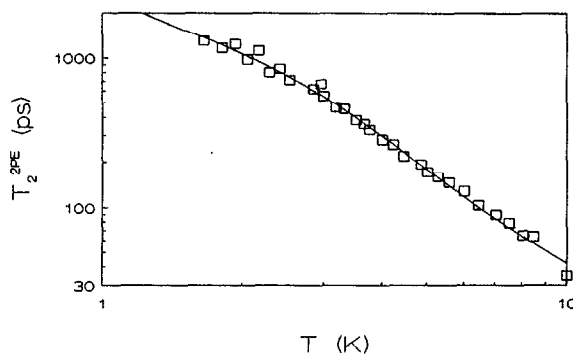


FIG. 13. The temperature dependence of the effective dephasing time derived from two pulse echo measurements in polymethylmethacrylate doped with pentacene. The fit has been made according to Eq. (12) using the parameters: $\alpha = 1.3 \pm 0.1$, $1/a = 2.8$ ns, $1/b = 14.4$ ps, $\Delta E = 15$ cm^{-1} , and $T_1 = 14$ ns.

for the activation energy was also found in photon echo studies on rhodamine B and octadecyl rhodamine B in PMMA.⁶⁶ The activation energy found in the echo experiments therefore seems to be caused by coupling of the chromophore to a specific mode of the polymer. Support for this interpretation is provided by Raman experiments on PMMA, which show a resonance at 13 cm^{-1} . A peak at this frequency was also found by Saikan *et al.*⁷² in hole burning experiments on meso-tetraphenylporphyrin doped into PMMA. Further experiments are needed to identify the precise nature of this local mode in the polymer.

VI. THE POPULATION DIMENSION OF THE 3PSE

So far the coherence dimension of the stimulated photon echo has been dealt with. The loss of optical coherence was measured as a function of the interval τ for a fixed waiting time t_w and this gave the effective homogeneous dephasing time $T_2(t_w)$. This last section will deal with the population dimension of the photon echo, in which the decay of the echo intensity is measured as a function of t_w for a constant pulse separation τ . Such a measurement monitors the depletion of the modulation depth of the frequency grating with a fixed spacing during the waiting time. This dimension of the stimulated echo yields information on population relaxation but is also very sensitive to spectral diffusion.

This last property of echo decay in the population dimension has been thoroughly explored in the study of spectral diffusion in electron spin echoes^{26,30} and phonon echoes.^{27,73} On the other hand, in the study of spectral diffusion in the optical domain most attention was focused on the decay of the coherence as measured by photon echoes²³ and or by hole burning.⁷⁴ However, Broer *et al.*⁷⁵ reported on experiments in a Nd^{3+} -doped silica fibre, where they measured the stimulated photon echo intensity as a function of t_w for a fixed τ . They observed a very fast initial decay in the first $20\text{ }\mu\text{s}$, which slowed down for longer t_w . The asymptotic decay time was in good agreement with the known fluorescence lifetime. The initial decay was faster for larger pulse separations τ and ascribed to spectral diffusion.

In Fig. 14 two typical echo decays in the population dimension of the 3PSE are shown for the system ZnP/EtOD at 1.5 K . The echo intensity is plotted as a function of the logarithm of the waiting time for two different pulse separations between the first and the second excitation pulses: $\tau=100\text{ ps}$ (squares) and $\tau=400\text{ ps}$ (circles). The data start at $t_w=12.5\text{ ns}$ and since the fluorescence lifetime of ZnP in EtOD is 2.7 ns at 1.5 K , the contribution of T_1 to the observed decay is small. At first sight the observed features in both decays are easily accounted for. From $t_w=10\text{ ns}$ to $1\text{ }\mu\text{s}$ the echo signal decreases due to the occurrence of spectral diffusion. The flat region from $1\text{ }\mu\text{s}$ to 1 ms arises from the gap in the distribution function of relaxation rates as observed in the "coherence" dimension of the 3PSE. In the millisecond time regime the signal drops sharply as a result of the combined effects of spectral diffusion and the limited bottleneck lifetime. The observation that the initial decay is faster for a larger pulse separation τ is also in agreement with assignment of this decay to spectral diffusion. The spacing of the frequency grating is inversely proportional to the time τ .

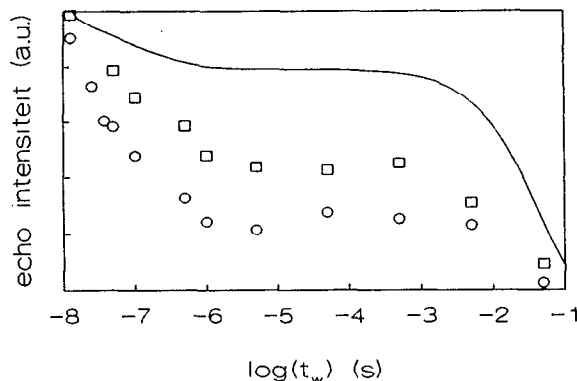


FIG. 14. Decay of the long-lived stimulated photon echo in deuterated ethanol doped with zincporphyrin at 1.5 K . The echo intensity has been monitored as a function of the waiting time t_w between the second and third excitation pulses (population dimension) for two different and fixed pulse separations τ between the first and second excitation pulses: $\tau=100\text{ ps}$ (squares) and $\tau=400\text{ ps}$ (circles). The solid line represents the calculated decay for $\tau=100\text{ ps}$ using Eq. (3).

The larger τ is, the finer the grating will be and the more this grating will be depleted by spectral diffusion.

Because the distribution of relaxation rates was already obtained from dephasing measurements, and the fluorescence and triplet-state lifetime as well as the intersystem crossing yield are known, it is also possible to calculate the stimulated photon echo decay resulting from spectral diffusion. The solid line in Fig. 14 is the theoretical decay curve for $\tau=100\text{ ps}$ based on the Hu and Walker Eq. (3) with the above-mentioned input parameters. Although the overall characteristics of the experimental and theoretical decay curves are similar, a remarkable difference exists in the slope of the curves in the time regime from ns to μs . In this time window the long-lived stimulated echo decays substantially faster than is predicted theoretically, even in case the intersystem crossing yield were to be significantly lower than reported.

The difference between experiment and a calculation based on measurements in the coherence dimension is even more striking for ZnP in TEA. In the previous sections it has already been demonstrated that in this system no spectral diffusion takes place in the time span ranging from $1\text{--}2\text{ ns}$ to 100 ms . This is confirmed by the measurements in the population dimension: the data in Fig. 15 for $\tau=100$ (crosses), 400 (triangles), and 500 ps (circles) are all coinciding. The calculated behavior represented by the solid line shows a slight decay in the ns regime, which is caused by the decay of the excited state. Afterwards, the curve is constant over the whole range of waiting times until the ms region where the decay is due to emptying of the bottleneck. Experimentally an additional decay of the echo from 100 ns to $1\text{ }\mu\text{s}$ is emphatically present and obviously not accounted for in the Hu and Walker theory of spectral diffusion.

As a final example of this anomalous echo decay, using a completely different chromophore, the data of pentacene in PMMA are presented in Fig. 16 together with the calculated decay. Once again, the experimental data exhibit in the $100\text{ ns--}1\text{ }\mu\text{s}$ region a faster decay than expected from a calcula-

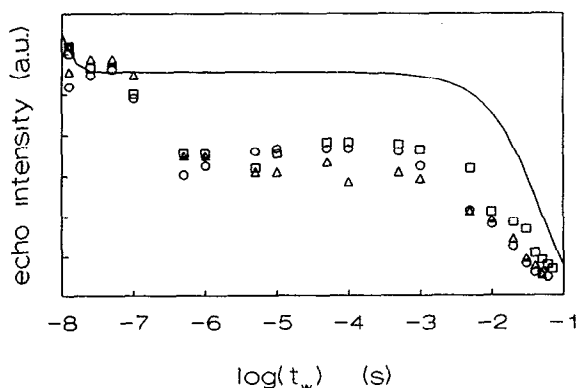


FIG. 15. Long-lived stimulated photon echo decay for zincporphyrin as guest molecule in a triethylamine glass at 1.5 K. The decay has been measured as a function of the waiting time t_w for different pulse separations τ between the first and second excitation pulses: $\tau=100$ ps (triangles), $\tau=400$ ps (circles), and $\tau=500$ ps (squares). The solid line is the calculated decay for $\tau=100$ ps using Eq. (3).

tion based on the distribution function of relaxation rates as measured in the dephasing dimension. Similar decays are (although not shown here) also found in the systems TZT in triethylamine, toluene, polystyrene, and polyvinylbutyral.

Unfortunately, the cause of the anomalous echo decay has not yet been identified, but in this section some possible suggestions for this phenomenon will be discussed. The most trivial explanation, namely, an artifact of the experimental setup, can immediately be excluded. As shown already above, long-lived stimulated echo measurements on the molecular mixed crystal pentacene in naphthalene provide no indication for a decrease of echo signal in the time window of interest. A fit to the stimulated photon echo decay yields values for the relaxation times which are in good agreement with earlier measurements on this system.^{71,76}

It has been proposed⁷⁷ that the noted discrepancy relates to the dynamics of the chromophore and not to the glass. For instance, the presence of another electronic state with a mi-

crosecond lifetime would explain the anomaly. However, there is no evidence that a state with such dynamical parameters exists in any of the metal porphyrins. Furthermore, the fact that the anomalous decay is found for all probes at the same time window between 100 ns and 1 μ s, including pentacene, which has a completely different molecular structure and dynamics, asks for a more general explanation.

It is clear that some additional relaxation mechanism has to exist, which introduces only a population relaxationlike process. This process must affect the modulation depths of both coarse and fine frequency gratings (small and large τ , respectively) in the same way, leaving the coherence dimension untouched. Large frequency jumps in a subset of chromophores, due to major structural changes in their environment would provide such a mechanism. If these jumps are much larger than the spacing of the frequency grating and become on the order of the bandwidth of the exciting laser frequency, then both coarse and fine gratings will indeed be affected to the same extent and only a decrease of the echo intensity in the population dimension will be observed.

Several options for the cause of the large frequency jumps are available. First, an intrinsic property of the chromophore could be responsible for the frequency shifts. In the process of relaxing from the excited electronic state to the bottleneck triplet state, energy is inevitably dumped in the surrounding medium of the chromophore. However, the long-lived echo is scattered from a *ground state* grating and consequently probes only the cold molecules. Nevertheless, it is possible that the energy, dumped by a nearby excited molecule, is the cause of an evolution of the glass structure in the neighborhood of the cold chromophore. A way to check out this intrinsic heating mechanism is to use an optical probe with a very long excited state lifetime or one that lacks a triplet state. A molecular radical therefore seems a perfect system with the bottleneck provided by the electron-nuclear spin states in the ground state.⁴¹ We have put considerable effort in echo experiments on the radicals *p*-xylyl and tri-(*p*-nitro-phenyl)-methyl but were not able to detect any photon echoes in these systems.

We propose that the noted discrepancy between theory and experiment signifies an inhomogeneity of the nonequilibrium glass structure, which is not accounted for in the standard treatment of the TLS model. The usual approach, is to assume that a chromophore is coupled to a sea of TLS's, and that consequently all chromophores can be treated on equal footing. However, considering the large inhomogeneous broadening in glasses, it is well conceivable that not all chromophores are coupled to the same set of TLS's because of their different local environment. In fact, the dissimilarity of the chromophores has recently been demonstrated by single molecule spectroscopy.⁷⁸ The optical linewidth of three different terrylene molecules doped in polyethylene showed a completely different temperature dependence, indicating that the local environment has a strong effect on dephasing and spectral diffusion. We suggest that in glasses a subset of chromophores is strongly coupled to a nearby TLS, perhaps in the first solvation shell of the impurity. Flipping of this TLS (an extrinsic one) induces a large frequency jump and will cause the anomalous decrease of the

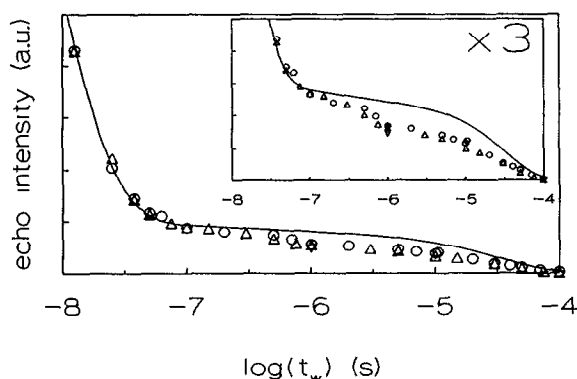


FIG. 16. Decay of the long-lived stimulated echo at 1.75 K in the system pentacene/polymethylmethacrylate as a function of the waiting time t_w while the interval τ between the first and second excitations is held constant at 70 ps. The circles and triangles represent measurements on different spots in the sample.

photon echo intensity. However, in order to test this hypothesis additional experiments are needed. In this regard it seems worthwhile to study glass dynamics with both single molecule spectroscopy and stimulated photon echo to investigate the cause of the breakdown of the standard TLS model for a full description of glass dynamics.

Furthermore, it is interesting to note here that we observed a discrepancy between the accumulated photon echo (APE) and 3PSE's in the sense that the effective T_2 obtained from an APE measurement is much longer than obtained from a 3PSE with a waiting time equal to the bottleneck life time of the chromophore. This implies that the effective accumulation time in an APE experiment, which should theoretically be equal to the triplet state life time, is much shorter than that. Instead, the effective accumulation time amounts to approximately 100 ns to 1 μ s for both ZnP/EtOD and pentacene/PMMA, which strongly suggests that a correlation with the anomalous 3PSE decay in the population dimension exists. Future experiments will be necessary to shine light on this problem.

VII. SUMMARY AND CONCLUSIONS

We have shown that the long-lived stimulated photon echo is ideal to map out the distribution function of fluctuation rates in amorphous solids over 11 decades, from THz to 10 Hz. From a comparison of the dynamics in several amorphous systems we have found evidence for the existence of two distinct TLS distributions in this time regime. From longitudinal photon echo measurements we also extract information on the population dynamics which suggests that chromophores are coupled to an inhomogeneous distribution of TLS's. The validity of the commonly used averaging procedure in the standard TLS model is questioned and should be further examined by combining single molecule spectroscopy with stimulated photon echo measurements.

ACKNOWLEDGMENTS

We wish to thank Dr. Otto T. Berg and Kees Lazonder for their assistance in some of the experiments and stimulating discussions. The investigations were supported by the Netherlands Foundations for Chemical Research (SON) and Physical Research (FOM) with financial aid from the Netherlands Organization for Scientific Research (NWO).

- ¹R. C. Zeller and R. O. Phol, *Phys. Rev. B* **4**, 2029 (1971).
- ²S. R. Elliot, *Nature (London)* **354**, 445 (1991).
- ³P. H. Gaskell, M. C. Eckersley, A. C. Barnes, and P. Chieux, *Nature (London)* **350**, 675 (1991).
- ⁴P. W. Anderson, B. I. Halperin, and C. M. Varma, *Philos. Mag.* **25**, 1 (1972).
- ⁵W. A. Phillips, *J. Low. Temp. Phys.* **7**, 351 (1972).
- ⁶M. T. Lopenen, R. C. Dynes, V. Narayanamurti, and J. P. Garno, *Phys. Rev. Lett.* **45**, 457 (1980).
- ⁷M. Meissner and K. Spitzman, *Phys. Rev. Lett.* **46**, 265 (1981).
- ⁸M. S. Love and A. C. Anderson, *J. Low. Temp. Phys.* **84**, 19 (1991).
- ⁹P. M. Selzer, D. L. Huber, D. S. Hamilton, W. M. Yen, and M. J. Weber, *Phys. Rev. Lett.* **36**, 813 (1976).
- ¹⁰R. M. Shelby, *Opt. Lett.* **8**, 88 (1983).
- ¹¹J. M. Hayes, R. P. Stout, and G. J. Small, *J. Chem. Phys.* **73**, 4129 (1980).
- ¹²J. M. Hayes, R. P. Stout, and G. J. Small, *J. Chem. Phys.* **74**, 4266 (1981).
- ¹³D. E. McCumber and M. D. Sturge, *J. Appl. Phys.* **34**, 1682 (1963).
- ¹⁴T. J. Aartsma and D. A. Wiersma, *Chem. Phys. Lett.* **42**, 520 (1976).
- ¹⁵H. P. H. Thijssen, A. I. M. Dicker, and S. Völker, *Chem. Phys. Lett.* **92**, 7 (1982).
- ¹⁶H. Fiddler, S. de Boer, and D. A. Wiersma, *Chem. Phys.* **139**, 317 (1989).
- ¹⁷J. Hegarty, M. M. Broer, B. Golding, J. R. Simpson, and J. B. MacChesney, *Phys. Rev. Lett.* **51**, 2033 (1983).
- ¹⁸B. L. Fear, R. P. Stout, J. M. Hayes, and G. J. Small, *J. Chem. Phys.* **78**, 7013 (1983).
- ¹⁹W. Breinl, J. Friedrich, and D. Haarer, *Chem. Phys. Lett.* **106**, 487 (1984).
- ²⁰C. A. Walsh, M. Berg, L. R. Narasimhan, and M. D. Fayer, *Chem. Phys. Lett.* **130**, 6 (1986).
- ²¹R. Wannemacher, J. M. A. Koedijk, and S. Völker, contribution to the International Conference on Luminescence, ICL'94, Stores, Connecticut.
- ²²K. A. Littau and M. D. Fayer, *Chem. Phys. Lett.* **176**, 551 (1991).
- ²³L. R. Narasimhan, Y. S. Bai, M. A. Dugan, and M. D. Fayer, *Chem. Phys. Lett.* **176**, 335 (1991).
- ²⁴W. E. Moerner and T. Basché, *Angew. Chem.* **32**, 457 (1993).
- ²⁵A. Zumbusch, L. Fleury, R. Brown, J. Bernard, and M. Orrit, *Phys. Rev. Lett.* **70**, 3584 (1993).
- ²⁶W. B. Mims, *Phys. Rev.* **168**, 370 (1968).
- ²⁷J. L. Black and B. I. Halperin, *Phys. Rev. B* **16**, 2879 (1977).
- ²⁸P. Hu and S. R. Hartman, *Phys. Rev. B* **9**, 1 (1974).
- ²⁹P. Hu and L. R. Walker, *Phys. Rev. B* **18**, 1300 (1978).
- ³⁰J. R. Klauder and P. W. Anderson, *Phys. Rev.* **125**, 912 (1962).
- ³¹Y. S. Bai and M. D. Fayer, *Chem. Phys.* **128**, 135 (1988).
- ³²J. M. Hayes and G. J. Small, *Chem. Phys.* **27**, 151 (1978).
- ³³R. van den Berg and S. Völker, *Chem. Phys. Lett.* **127**, 525 (1986).
- ³⁴H. de Vries and D. A. Wiersma, *J. Chem. Phys.* **72**, 1851 (1980).
- ³⁵K. A. Littau, A. Elschner, and M. D. Fayer, *Chem. Phys. Lett.* **175**, 149 (1990).
- ³⁶S. Saikan, J. W.-I. Lin, and H. Nemoto, *Phys. Rev. B* **46**, 7123 (1992).
- ³⁷J. Zollfrank, J. Friedrich, J. M. Vanderkooi, and J. Fidy, *J. Chem. Phys.* **95**, 3134 (1991).
- ³⁸H. van der Laan, Th. Schmidt, R. W. Visschers, K. J. Visscher, R. van Grondelle, and S. Völker, *Chem. Phys. Lett.* **170**, 231 (1990).
- ³⁹D. Thorn Leeson, O. T. Berg, and D. A. Wiersma, *J. Phys. Chem.* (accepted for publication).
- ⁴⁰R. Wannemacher, J. M. A. Koedijk, and S. Völker, *Chem. Phys. Lett.* **206**, 1 (1993).
- ⁴¹J. B. W. Morsink, W. H. Hesselink, and D. A. Wiersma, *Chem. Phys. Lett.* **64**, 1 (1979).
- ⁴²H. C. Meijers and D. A. Wiersma, *Phys. Rev. Lett.* **68**, 381 (1992).
- ⁴³B. Herzog and E. L. Hahn, *Phys. Rev.* **103**, 148 (1956).
- ⁴⁴J. B. W. Morsink, W. H. Hesselink, and D. A. Wiersma, *Chem. Phys. Lett.* **71**, 289 (1982).
- ⁴⁵D. L. Huber, M. M. Broer, and B. Golding, *Phys. Rev. Lett.* **52**, 2281 (1984).
- ⁴⁶R. Maynard, R. Rammal, and R. Suchail, *J. Phys. (Paris)* **41**, L291, L614 (1980).
- ⁴⁷Y. S. Bai and M. D. Fayer, *Phys. Rev. B* **39**, 11 066 (1989).
- ⁴⁸J. Jäckle and K.-L. Jüngst, *Z. Phys. B* **30**, 243 (1978).
- ⁴⁹J. C. Lasjaunias, A. Ravex, M. Vandorpe, and S. Hunklinger, *Solid State Commun.* **17**, 1045 (1975).
- ⁵⁰Th. Schmidt, J. Baak, D. A. van de Straat, H. B. Brom, and S. Völker, *Phys. Rev. Lett.* **71**, 3031 (1993).
- ⁵¹R. Jankowiak and G. J. Small, *Chem. Phys. Lett.* **207**, 436 (1993).
- ⁵²W. H. Hesselink and D. A. Wiersma, *Chem. Phys. Lett.* **56**, 227 (1978).
- ⁵³W. H. Hesselink, Thesis, University of Groningen, 1980.
- ⁵⁴H. Stehfest, *Commun. ACM* **13**, 47 (1970).
- ⁵⁵K. A. Littau, M. A. Dugan, S. Chen, and M. D. Fayer, *J. Chem. Phys.* **96**, 3484 (1992).
- ⁵⁶P. J. van der Zaag, J. P. Galaup, and S. Völker, *Chem. Phys. Lett.* **166**, 263 (1990).
- ⁵⁷M. B. Weissman, *Rev. Mod. Phys.* **60**, 537 (1988).
- ⁵⁸H. C. Meijers and D. A. Wiersma, *J. Lumin.* **53**, 80 (1992).
- ⁵⁹O. Haida, H. Suga, and S. Seki, *J. Chem. Therm.* **9**, 1133 (1977).
- ⁶⁰M. D. Fayer (private communication).
- ⁶¹R. Jankowiak and G. J. Small, *Phys. Rev. B* **47**, 14 805 (1993).
- ⁶²R. Jankowiak, G. J. Small, and K. B. Athreya, *J. Phys. Chem.* **90**, 3896 (1990).
- ⁶³L. Fleury, J. Bernard, R. Brown, and M. Orrit, contribution to the conference DPC'93, Cambridge, Massachusetts.
- ⁶⁴B. Jackson and R. Silbey, *Chem. Phys. Lett.* **99**, 331 (1983).

- ⁶⁵ S. Völker, *Relaxation Processes in Molecular Excited States* (Kluwer Academic, Dordrecht, 1989), and references therein.
- ⁶⁶ A. Elschner, L. R. Narasimhan, and M. D. Fayer, *Chem. Phys. Lett.* **171**, 19 (1990).
- ⁶⁷ D. Hsu and J. L. Skinner, *J. Chem. Phys.* **81**, 5471 (1984).
- ⁶⁸ R. Wannemacher, H. E. Smorenburg, Th. Schmidt, and S. Völker, *J. Lumin.* **53**, 266 (1993).
- ⁶⁹ H. van der Laan, H. E. Smorenburg, Th. Schmidt, and S. Völker, *J. Opt. Soc. Am. B* **9**, 931 (1992).
- ⁷⁰ L. W. Molenkamp and D. A. Wiersma, *J. Chem. Phys.* **83**, 1 (1985).
- ⁷¹ H. C. Meijers, Thesis, University of Groningen, 1994.
- ⁷² S. Saikan, T. Kishida, Y. Kanematsu, H. Aota, A. Harada, and M. Kamachi, *Chem. Phys. Lett.* **166**, 358 (1990).
- ⁷³ B. Golding and J. E. Graebner, *Phys. Rev. Lett.* **37**, 852 (1976).
- ⁷⁴ *J. Lum.* **36**, 1 (1986), Special issue *Optical Linewidths in Glasses*.
- ⁷⁵ M. M. Broer, B. Golding, W. H. Haemmerle, J. R. Simpson, and D. L. Huber, *Phys. Rev. B* **33**, 4160 (1986).
- ⁷⁶ W. H. Hesselink, Thesis, University of Groningen, 1980.
- ⁷⁷ A. Suarez and R. J. Silbey (private communication).
- ⁷⁸ L. Fleury, A. Zumbusch, M. Orrit, R. Brown, and J. Bernard, *J. Lumin.* **56**, 15 (1993).